

**PETROLOGY OF ASTEROID RYUGU PARTICLES ALLOCATED TO THE PHASE2 CURATION KOCHI TEAM.** A. Yamaguchi<sup>1,2</sup>, M. Kimura<sup>1</sup>, M. Ito<sup>3</sup>, N. Tomioka<sup>3</sup>, M. Uesugi<sup>4</sup>, N. Imae<sup>1,2</sup>, N. Shirai<sup>5</sup>, T. Ohigashi<sup>6,2</sup>, M-C. Liu<sup>7</sup>, R. C. Greenwood<sup>8</sup>, K. Uesugi<sup>4</sup>, A. Nakato<sup>9</sup>, K. Yogata<sup>9</sup>, H. Yuzawa<sup>6</sup>, Y. Kodama<sup>†</sup>, A. Tsuchiyama<sup>10</sup>, M. Yasutake<sup>4</sup>, R. Findlay<sup>8</sup>, I. A. Franchi<sup>8</sup>, J. A. Malley<sup>8</sup>, K. A. McCain<sup>7</sup>, N. Matsuda<sup>7</sup>, K. D. McKeegan<sup>7</sup>, K. Hirahara<sup>11</sup>, A. Takeuchi<sup>4</sup>, S. Sekimoto<sup>12</sup>, I. Sakurai<sup>13</sup>, I. Okada<sup>13</sup>, Y. Karouji<sup>14</sup>, T. Yada<sup>9</sup>, M. Abe<sup>9</sup>, T. Usui<sup>9</sup>, S. Watanabe<sup>13</sup>, and Y. Tsuda<sup>2,14</sup>. <sup>1</sup>NIPR (Tokyo 190-8518, Japan, yamaguch@nipr.ac.jp), <sup>2</sup>SOKENDAI, <sup>3</sup>KOCHI, JAMSTEC, <sup>4</sup>JSRI/SPring-8, <sup>5</sup>TMU, <sup>6</sup>UVSOR IMS, <sup>7</sup>UCLA, <sup>8</sup>Open Univ., <sup>9</sup>ISAS JAXA, <sup>10</sup>Ritsumeikan Univ., <sup>11</sup>Osaka Univ., <sup>12</sup>Kyoto Univ., <sup>13</sup>Nagoya Univ., <sup>14</sup>JAXA, <sup>†</sup>Now at Toyo Corp.

**Introduction:** C-type asteroids, the sources of carbonaceous chondrites, are remnants of primitive planetesimals that existed in the early Solar System. The Hayabusa2 spacecraft collected surface and subsurface samples from the C-type asteroid Ryugu [1], which provide the clues to understand the evolution of early Solar System materials. Here, we report the petrology of Ryugu particles and discuss their formation history in order to better understand the early evolutionary processes that occurred on Ryugu. This work is part of a series of studies, including mineralogy and petrology, high precision oxygen isotopes and SIMS analyses of anhydrous minerals and carbonates of the particles allocated to Phase2 curation Kochi [2-7].

**Experimental Methods:** We made polished sections of five particles (A0029, A0037, C0009, C0014, and C0068) for our petrologic study. The particles were chipped or cut by a diamond wire saw and then embedded in epoxy in dry nitrogen. Potted butts of the samples were polished with only a diamond lapping sheet under air, without using any fluid and finished with a 0.5  $\mu\text{m}$  diamond sheet. We examined these polished sections using an optical microscope and a field emission scanning electron microscope (FE-SEM; JEOL JSM-7100F) equipped with an energy dispersive spectrometer (Oxford AZtec Energy) and an electron microprobe analyzer (EPMA; JEOL JXA-8200) at NIPR. The beam current used for observations was <1 nA to avoid electron damage to the surfaces. Phyllosilicates and matrix materials were analyzed with a current of 5 nA and a focused beam, carbonates and phosphates with a 5 nA defocused beam ( $\sim 5 \mu\text{m}$  in diameter), olivine, pyroxene, magnetite and sulfides were measured with a 30 nA, focused beam, all at 15 keV. Natural and synthetic materials were used as standards. Data were reduced using a ZAF correction program.

**Results and discussion:** The polished sections (areas = 0.9–4.2 mm<sup>2</sup>) consist of phyllosilicate (64–88 vol%), magnetite (4–7 vol%), sulfide minerals (3–6 vol%), carbonate (2–23 vol%) with minor amounts of anhydrous silicates (olivine and pyroxene), chromite,

spinel, apatite, and Na-Mg phosphate. The particles from Chamber A have more pore spaces (9–14 vol%) than those from Chamber C (2–4 vol%), consistent with the brittle nature of Chamber A particles during sample processing. The bulk compositions determined by a broad-beam ( $\sim 30 \mu\text{m}$  in diameter) analysis by EPMA and by INAA [3] are CI-like except for Ca and Mn due to the heterogeneous distribution of carbonates. The petrology and mineralogy of the particles are very similar to CI chondrites [e.g., 8].

The particles we studied are dominated by a fine-grained matrix and contain subrounded to irregular phyllosilicate-rich clasts and mineral grains (fragments?) of sulfides, magnetite, and other minor minerals (Fig. 1). There are textually slightly different lithologies. Sulfide-rich lithologies (clasts?) are irregular in shape (several tens of  $\mu\text{m}$ ) and contain abundant tiny grains of sulfides. A dolomite-rich lithology occurs in A0037 and includes abundant, large dolomite grains. A phosphate-rich lithology contains lots of apatite up to a few tens of  $\mu\text{m}$ . We found a subrounded object that contains angular olivine. This object might be the relict of a chondrule.

Phyllosilicate clasts show a feathery, fibrous texture (Fig. 1). Some of the clasts are plain (featureless). The boundaries between the clasts and matrix are not always clear. In some cases, coarse-grained phyllosilicates are in contact with dolomites. Coarse-grained phyllosilicates also occur as veins or elongated objects mixed with the matrix. In contrast, matrix phyllosilicate is finer-grained (textures invisible by FE-SEM) and intimately mixed or surrounded by tiny sulfide grains.

We found three carbonate minerals, dolomite, Ca carbonate, and breunnerite. Dolomite is the most common phase and occurs ubiquitously. Dolomite is exceptionally rich in A0037 (21 vol%) (the dolomite-rich lithology). These dolomite grains in A0037 have oscillatory zoning of Mn, Fe and Ca. The zoned dolomite grains are fragmented, indicating impact events. Ca carbonate is only found in C0009. Some of the Ca carbonate form chains of grains, while others are scattered in the matrix. This indicates that Ca carbonate originally formed as veins and was later brecciated. We

found one dolomite in contact with breunnerite in C0009.

There are two occurrences of sulfide minerals. First, large, euhedral (lath or hexagonal) to subhedral grains of sulfides occur in the matrix. Many are partially corroded. Secondly, tiny (<1  $\mu\text{m}$ ) grains of sulfides (pyrrhotite, pentlandite) [4] occur in the matrix and as chains that surround fine phyllosilicate fragments in the matrix. Similarly, pyrrhotites also occur as rims to phyllosilicate clasts and Ca carbonate. These textures indicate that the fine-grained sulfides may have formed by later sulfidization after brecciation. Pentlandite also occurs as grains in the matrix and as tiny (<several  $\mu\text{m}$ ) inclusions in pyrrhotite. We found large grains (<80  $\mu\text{m}$ ) of cubanite in C0014. Comparison between the chemical compositions of the sulfides and phase diagrams [9] indicates that these sulfide minerals formed at low temperatures ( $\sim 25^\circ\text{C}$ ).

Magnetite occurs as framboids, platelets and spherulitic grains, similar to those found in CI chondrites [e.g., 10]. Spheroidal magnetite shows a fan-spherulitic texture. They occur in isolated grains in the matrix, as well as inclusions in dolomite.

We found several olivine and pyroxene fragments in C0009. A few of them show a porous texture. In some cases, the rims of the fragments are replaced by fibrous phyllosilicates suggesting partial aqueous alteration. Most of the olivine grains are Mg-rich ( $\text{Fa}_{0.8-4.6}$ ,  $\text{FeO/MnO}$  (wt%/wt%) = 1.4–39.0). Because of the aqueously altered textures and compositions, they are likely to be indigenous to Ryugu, rather than xenolithic materials. The Mg-rich olivine grains with low  $\text{FeO/MnO}$  could be related to AOAs [11].

Ca-phosphate is scattered throughout the matrix and contains traces of F (0.2–0.7 wt%) and Cl (<0.1 wt%), indicating they are hydroxyapatite. Na-Mg-rich phosphates ( $\sim 5$ –6 wt% Na;  $\sim 20$  wt% Mg) occur as veins (<several  $\mu\text{m}$  thick) in the matrix. They are aggregates of thin sheet-like materials. They have not been found in CI chondrites. Small grains of spinel, chromite and carbonaceous materials are present in the matrix.

Bulk chemical compositions and the presence of relict anhydrous silicates and chondrules indicate that the precursor material to the Ryugu grains was chondritic and accreted with ice. Internal heating by the decay of  $^{26}\text{Al}$  caused melting of ice and aqueous alteration within the parent body. It is unlikely that chondritic textures were solely destroyed by aqueous alteration, instead the protolith was probably brecciated by impact events. It is difficult to constrain the relative chronology from the petrologic observations. Because dolomite often contains grains of magnetite, and fine-grained phyllosilicate silicates occur interstitially, dolomite formed after the formation of phyllosilicate

matrix and magnetite. Magnetite formation may have predated the formation of the large pyrrhotite because one of the large pyrrhotite grains contains magnetite inclusions. Na-Mg-rich phosphate veins formed after the formation of the matrix. The final brecciation event fragmented large dolomite grains. We conclude that the Ryugu asteroid experienced multi-stage processing, including aqueous alteration, brecciation, and Na-P metasomatism.

Preliminary results of in-situ oxygen isotopic analysis with SIMS in anhydrous minerals (i.e., olivine and pyroxene) in C0009 section and secondary phases (dolomites, Ca carbonate and magnetite) in both A0037 and C0009 sections are presented in this conference [6,7]. In combination with the detailed mineralogical descriptions, isotopic studies will give a critical insight into the evolutionary history of the asteroid Ryugu.

#### References:

- [1] Yada T. et al. (2021) *Nature Astron.*, doi.org/10.1038/s41550-021-01550-6. [2] Ito M. et al. (2020) *Earth Planets Space*, 72, 133. [3] Ito M. et al. (2022) *53<sup>rd</sup> LPSC*. [4] Tomioka N. et al. (2022) *53<sup>rd</sup> LPSC*. [5] Greenwood R. C. et al. (2022) *53<sup>rd</sup> LPSC*. [6] Liu M-C. et al. (2022) *53<sup>rd</sup> LPSC*. [7] McCain K. A./Matsuda N. et al. (2022) *53<sup>rd</sup> LPSC*. [8] Tomeoka K. and Buseck P. (1988) *Geochim. Cosmochim. Acta.*, 52, 1627–1640. [9] Berger E. L. et al. (2016) *Meteorit. Planet. Sci.*, 51, 1813–1829. [10] Kerridge J. F. et al. (1979) *Science* 205, 395–397. [11] Komatsu M. et al. (2015) *Meteorit. Planet. Sci.*, 50, 1271–1294.

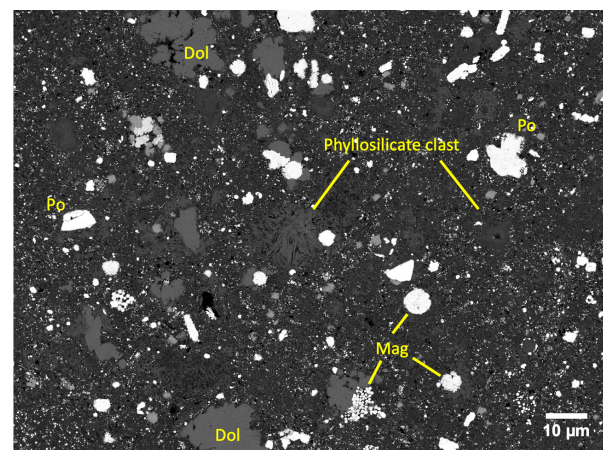


Fig. 1. Back-scattered electron image of C0014. Phyllosilicate clasts, fragments of pyrrhotite (Po), dolomite (Dol), and magnetite (Mag) are set in a fine-grained matrix.